MINERALOGICAL JOURNAL, VOL. 11, NO. 7, PP. 317-330, JULY, 1983

Syntheses and superstructures of $(Cd, M)_5(PO_4)_3OH$ (M=Mn, Fe, Co, Ni, Cu, Hg)

Mayumi HATA and Fumiyuki MARUMO

Research Laboratory of Engineering Materials, Tokyo Institute of Technology, Nagatsuta 4259, Midori-ku, Yokohama 227, Japan

Abstract

Divalent ions of the first series transition elements and Hg were introduced into a cadmium hydroxyapatite $Cd_5(PO_4)_3OH$ by replacing a part of Cd^{2+}, and the effects on the crystal growths and the structural changes were studied. Cd^{2+} can be exchanged with Mn^{2+} up to about 30 mol %, with Ni^{2+} or Hg^{2+} up to about 10 mol %, and with a little amount of Fe^{2+} or Cu^{2+}. It was found that $Cd_5(PO_4)_3OH$ forms a superstructure when it contains a small amount of Mn^{2+}, Fe^{2+}, Co^{2+}, Ni^{2+}, Cu^{2+} or Hg^{2+} ion. Infrared spectra of $Cd_5(PO_4)_3OH$ containing these ions show some new bands in addition to those of $Cd_5(PO_4)_3OH$. The average structures of the crystals containing a small amount of Hg^{2+} and Ni^{2+}, and the superstructure of the crystal containing Mn^{2+} were refined with the full-matrix least-squares method, although the amounts and sites of the substituting ions could not be determined except for the crystals containing Hg^{2+}. The superstructure belongs to $P6_3$ (a=16.1990(3), c=6.6485(1) Å and Z=6) and has more distorted PO_4 tetrahedra than the structure of pure $Cd_5(PO_4)_3OH$.

Introduction

Since Náray-Szabó (1930) and Mehmel (1930) determined the crystal structure of apatite independently, many works have been reported on the structure of apatite group compounds. Most of them belong to the hexagonal, centrosymmetric space group $P6_3/m$. A few of them belong to the monoclinic space group $P2_1/b$ and transform into the hexagonal $P6_3/m$ phase at about 200°C (Prener, 1967). Although apatite is known to contain many kinds of atoms substituting for Ca, P or F, few kinds of divalent transition elements constitute the apatite structure. The smallest metallic ion which forms chlorapatite is Mn^{2+} (Kreider and Hummel, 1970), and that which forms hydroxyapatite is Cd^{2+} (Hata *et al.*, 1978). The ionic sizes of Mn^{2+} and Cd^{2+} are thought to be the lower limits of the ionic sizes to form chlorapatite and hydroxyapatite, respectively. The divalent

* Present address: Gifu College of Dentistry, Takano, Hozumi-cho, Motosu-gun, Gifu 501-02, Japan

ions of the first series transition elements have slightly smaller ionic radii (Shannon, 1976) than that of Cd^{2+} and are essential elements for human body.

Taking into account these facts, $Cd_5(PO_4)_3OH$ were synthesized under the presence of Mn^{2+}, Fe^{2+}, Co^{2+}, Ni^{2+}, Cu^{2+} or Hg^{2+}. The products were examined with the X-ray diffraction method, infrared spectroscopy and electron-probe micro-analysis. Since it was difficult to synthesize single crystals of calcium hydroxyapatite containing enough amounts of these ions to use for single crystal X-ray diffraction studies, $Cd_5(PO_4)_3OH$ was used in place of $Ca_5(PO_4)_3OH$. It was revealed that the crystal growth of $Cd_5(PO_4)_3OH$ is influenced by these ions and that the crystal forms a superstructure with the space group $P6_3$ on incorporation of a small amount of these ions. In the average stucture, three out of four oxygen atoms of the PO_4^{3-} group show remarkably anisotropic thermal vibrations.

Synthesis of crystals

$Cd_5H_2(PO_4)_4 \cdot H_2O$ used as the starting material was precipitated from solution; 0.1 mol/l solutions of $Cd(NO_3)_2 \cdot 4H_2O$ and H_3PO_4 were mixed so that the molar ratio of Cd and PO_4 becomes 5 : 4. The pH of the suspension was controlled to about 5.0 by adding 0.5 N NaOH solution. Crystals were synthesized by a hydrothermal reaction; 0.05 g of $Cd_5H_2(PO_4)_4 \cdot 4H_2O$, various amounts of nitrates of Mn^{2+}, Co^{2+}, Ni^{2+} Cu^{2+} or Hg^{2+}, or Mohr's salt, and 5 ml of distilled water were mixed in glass ampules of about 7 cm^3 in volumes. The initial pH of each suspension was in the range 5.5–7.0. Each ampule was sealed and set in a silicon oil bath. The hydrothermal reaction was performed at about 200°C for 2 weeks. The pH values of the residual solutions after the reactions were in the range 2.5–4.0.

The tolerance of $Cd_5(PO_4)_3OH$ for the elements mentioned above was found to be small. A good deal of coexistent ions inhibit the precipitation of $Cd_5(PO_4)_3OH$ by forming other phosphates. Mn^{2+} substitutes for Cd^{2+} up to about 30 mol %, Ni^{2+} and Hg^{2+} substitute for it up to about 10 mol %, and Fe^{2+} and Cu^{2+} only slightly under the condition employed in this study. (These values were estimated by EPMA.) Fe^{2+} and Cu^{2+} could not be detected by EPMA on the specimens grown under existence of these ions, though the crystals were tinged with blue. Analysis of Co^{2+} was not carried out, because crystals synthesized under existence of Co^{2+} were too thin to arrange for EPMA measurement. Mn^{2+} and Ni^{2+} ions were found to be distributed often by forming sector zoning on line scanning of electron probe. Especially zoning of Mn^{2+} distribution was distinct.

Impurity effect of transition elements and Hg^{2+} ions on the growth form of $Cd_5(PO_4)_3OH$ was observed; when these ions do not exist, $Cd_5(PO_4)_3OH$ crystals grow into hexagonal prisms with the sizes about 0.1–0.2 mm after the hydrothermal reaction at about 200°C for 2 weeks under the pH region 3.0–7.0. Whereas, they grow into short hexagonal prisms with the sizes up to 0.5 mm, when Mn^{2+}, Cu^{2+} or Hg^{2+} exists, and existence of Fe^{2+}, Ni^{2+} or Co^{2+} leads to a habit of thin hexagonal plates with the sizes of around 0.1 mm under the same hydrothermal condition.

Infrared absorption spectroscopy

Infrared absorption runs of cadmium hydroxyapatite containing Mn^{2+}, Fe^{2+}, Ni^{2+} Cu^{2+}, or Hg^{2+} were carried out in the range 4000 to 250 cm^{-1}. 100 mg of CsI and 2–3 mg of powdered apatite crystals were pressed in an evacuated die under a total force of 5 tons for 7 min. Spectra were recorded using HITACHI 295 spectrometer with the powdered samples suspended in CsI under the 50% relative humidity of atmosphere. The infrared spectra of $Cd_5(PO_4)_3OD$, $Cd_5(PO_4)_3Cl$ and $Ca_5(PO_4)_3OH$ and those containing Mn^{2+} or Cu^{2+} were also recorded in the same region, for the sake of assignment.

The products showed essentially the same spectra as $Cd_5(PO_4)_3OH$, showing several new bands at 1220, 800, 760, 480 and 460 cm^{-1} in addition to those of $Cd_5(PO_4)_3OH$. The band intensity at 760 cm^{-1} is strongest among these new bands. The infrared spectra of $Cd_5(PO_4)_3OH$ and those containing a small amount of Mn^{2+} and Cu^{2+}, and of their deuterated analogues are shown in Fig. 1. Spectra of the deuterated samples indicate nearly 100% OD substitution as estimated from reduction in OH librational and stretching modes. All of the additional bands did not shift on OD substitution.

Crystal structure analysis

Crystals of cadmium hydroxyapatite containing Mn^{2+}, Fe^{2+}, Co^{2+}, Ni^{2+}, Cu^{2+} or Hg^{2+} were revealed to have superstructures by the single-crystal X-ray diffraction method. From Weissenberg and precession photographs, all crystals were found to have the Laue symmetry $6/m$ with systematic absences of $00l$ for l odd. The lattice vectors of the superstructure are expressed in terms of its subcell vectors $\mathbf{a}_s$, $\mathbf{b}_s$, $\mathbf{c}_s$ by the following relations,

$$\mathbf{a}=\mathbf{a}_s-\mathbf{b}_s,$$

$$\mathbf{b}=\mathbf{a}_s+2\mathbf{b}_s,$$

$$\mathbf{c}=\mathbf{c}_s.$$

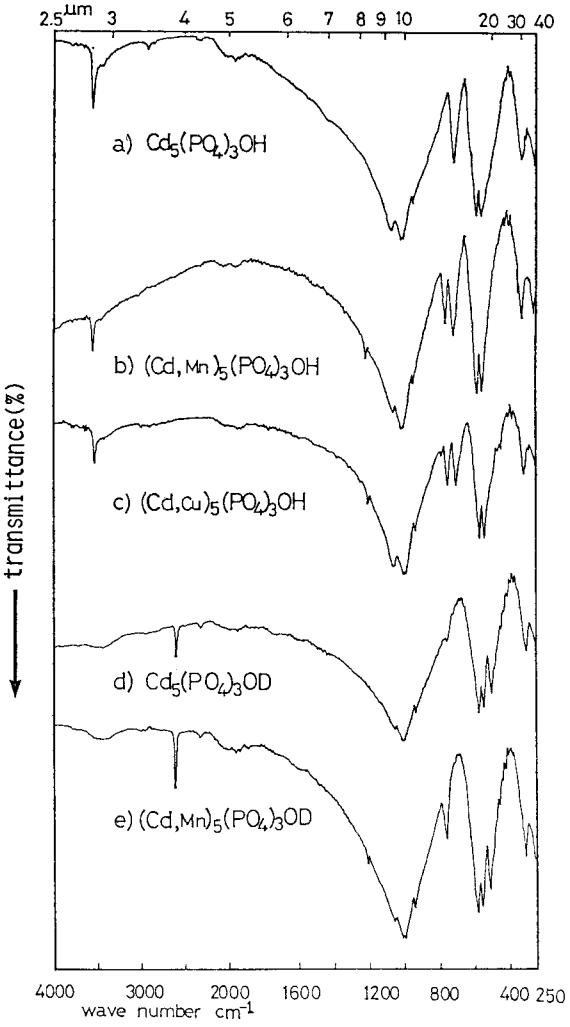

FIG. 1. Infrared spectra of various cadmium apatites.

The possible space groups are restricted to $P6_3/m$ (centrosymmetric) and $P6_3$ (non-centrosymmetric). The *hkl* precession photograph is given in Fig. 2, and the relation of the unit cells between the average structure and superstructure is shown in Fig. 3.

Intensity measurements were carried out for two pale brown crystals with hexagonal prismatic shapes and different depths of color due to Hg^{2+} (crystals A and B), a yellow, hexagonal prismatic crystal containing a small amount of Ni^{2+} (crystal C) and for a pink, hexagonal prismatic crystal containing a small

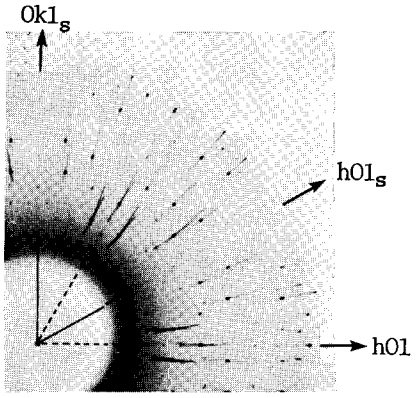

FIG. 2. The hkl precession photograph of superstructure.

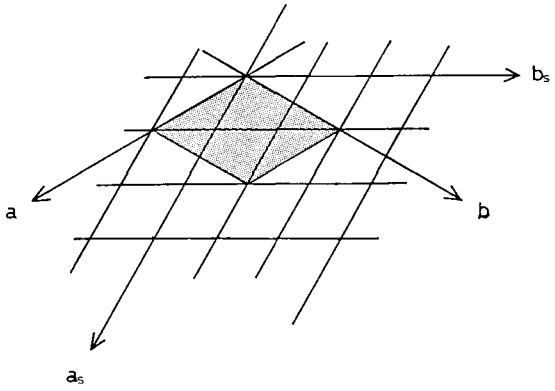

FIG. 3. Unit cells of the superstructure and average structure.

amount of Mn^{2+} (crystal D), on automated four-circle diffractometers (Philips PW 1100/20 for crystals A and B, Rigaku AFC-5 for crystals C and D) in the 2θ-ω scan mode, with a scan speed of 2°/min in ω, using MoKα radiation. The dimensions of the crystals, the numbers of independent reflection data $[|F_o|>3\sigma(|F_o|)]$ and 2θ ranges are tabulated in Table 1. For the crystal D, 746 are the superlattice reflections.

The lattice constants of the crystals A, B, C and D were obtained with the program RLC3 (Sakurai, 1967) from the 2θ values of 21, 27, 29 and 29 reflections measured on the automated four-circle diffractometers, respectively. These values are listed in Table 2.

The chemical analyses of these four crystals were not performed. However, the presence of Hg in the crystals A and B was confirmed as follows. Crystals

TABLE 1. Data on intensity collection and the final R values.

Crystal	Crystal size (mm)	Range of 2θ	number of reflections	R(%)	R_w(%)
A	$0.20\phi \times 0.10$	<90	1255	5.85	7.30
B	$0.05\phi \times 0.22$	<90	1089	3.49	3.92
C	$0.05\phi \times 0.15$	<90	1057	3.36	3.62
D	$0.15\phi \times 0.15$	<75	1532	3.00	3.34

TABLE 2. Cell dimensions. Values for crystals A, B, C are those of sub-cell. For comparison, those values for pure $Cd_5(PO_4)_3OH$ are listed.

Crystal	a (Å)	c (Å)
$Cd_5(PO_4)_3OH$	9.335 (2)	6.664 (3)
A	9.335 (2)	6.666 (1)
B	9.348 (3)	6.660 (1)
C	9.3440(2)	6.6655(2)
D	16.1990(3)	6.6485(1)

tinged with brown were picked up from the same batch as the crystals A and B came from. Then the average Hg and Cd contents of these crystals were determined by means of atomic absorption analysis by Mr. H. Sakamoto of Kagoshima University, giving the values Hg : 6.84 and Cd : 44.8 wt %. Crystals tinged with pale brown were also picked out from the same batch, and atomic absorption analysis was carried out, yielding the results Hg : 2.26 and Cd : 48.9 wt %. These facts as well as the results of EPMA certify the presence of Hg in the crystals A and B, Ni in the crystal C and Mn in the crystal D.

Intensities were corrected for Lorentz and polarization factors. Absorption correction ($\mu = 10.9\ mm^{-1}$ for MoKα) were also applied by taking the crystal shapes into consideration. Since the intensities of superlattice reflections were too weak in the crystals A, B and C to analyze the superstructures, only the average structures were determined for these crystals, and the superstructure was analyzed only on the crystal D containing Mn.

The refinements of the average structures were started by assuming the composition of the ideal $Cd_5(PO_4)_3OH$ and the parameters of the Cd(1) and Cd(2) atoms in the structure of $Cd_5(PO_4)_3OH$ for the Cd atoms with intensity data of the main reflections which satisfy the relation $h-k=3n$. The positions of P and O atoms were determined from the subsequent difference Fourier synthesis, and the parameters were refined with the full-matrix least-squares program LINUS (Coppens and Hamilton, 1970). The populations of the Cd, Hg, Ni and Mn atoms at the sites Cd(1) and Cd(2) were varied in the course of the refinements. The calculation on the crystals A and B revealed that Hg exchanges

only the Cd(1) atoms accompanying vacancies, whereas no evidence of cation substitutions was obtained on the crystals C and D from the population analyses. Therefore, populations of the cations at the Cd(1) site were varied in the subsequent refinements of the crystals A and B, and the Cd(1) and Cd(2) sites were assumed to be fully occupied by Cd in the crystals C and D, by neglecting the contributions of Ni and Mn. The populations of Cd(1) and Hg atoms converged to 0.60(4) and 0.22(2) in the crystal A and to 0.80(2) and 0.12(2) in B, respectively. The final R and R_w values are given in Table 1, where R_w is in the form $\Sigma w(|F_o|-|F_c|)^2/\Sigma|F_o|^2$. The weighting scheme employed was that of Hughes' (Hughes, 1941). In the refinements, the space group $P6_3/m$ was assumed and anisotropic thermal parameters were applied for all the atoms. All of the obtained positional and thermal parameters are approximately equal to those of $Cd_5(PO_4)_3OH$ (Hata *et al.*, 1978). The thermal ellipsoids for the crystal A are shown in Fig. 4 with the program DCMS3 (Takenaka, 1972), enclosing 50% probability.

The partial Patterson maps based only on the superlattice reflections of the crystal D showed several quadruplets indicating small deviations of Cd atoms from the averaged positions (Fig. 5). The deviation of each atom was estimated by the program KEY (Ito, 1973). Remarkable deviations in the z direction suggested the non-centrosymmetric space group $P6_3$ for the superstructure.

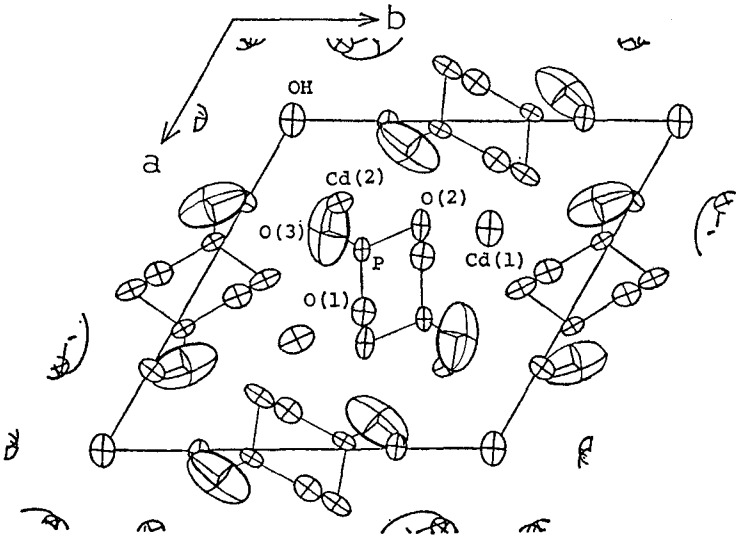

FIG. 4. The average structure projected on (001). The thermal ellipsoids are scaled to enclose 50% probability. One of the O(3) atoms which are related by a mirror plane are neglected.

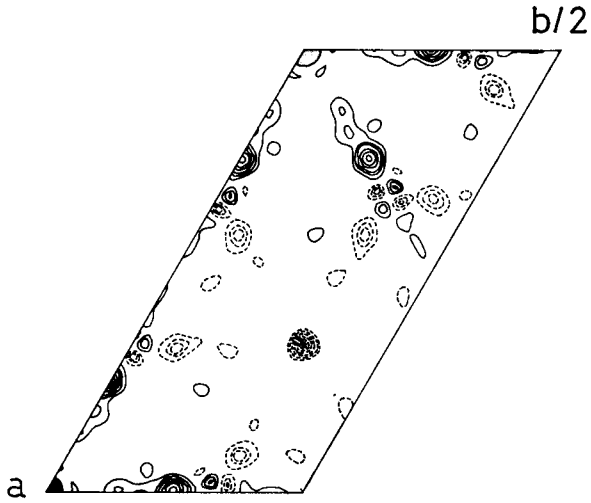

FIG. 5. A partial Patterson map on the plane $z=0$. Contours are at an interval of $0.2\,e^2/Å^3$ and the first positive contour is at $0.1\,e^2/Å^3$. Negative electron density is indicated by broken contours.

Refinement of the superstructure was started with the positional parameters obtained by KEY. Each of the crystallographically independent atoms except Cd(1) in the average structure splits into three independent atoms in the superstructure, which are originally related with the translational symmetry. They are labelled with A, B or C in the present paper. The Cd(1), O(3) and O(H) atoms have crystallographically equivalent atoms related with a mirror plane in the average structure. These atoms become independent in the superstructure, and designated by adding a label A or B in the case of Cd(1) and a prime (′) in O(H). The O atom originally related to O(3) with the mirror plane is denoted as O(4). The positional and thermal parameters for all the atoms except O(HA)′ and O(HC)′, which were fixed, were refined with the full-matrix least-squares program LINUS. The electron densities observed in the Fourier maps around the positions of O(H) and O(H)′ [O(HA) and O(HA)′, O(HB) and O(HB)′, O(HC) and O(HC)′], which are related by the mirror plane in the average structure, are different each other. The optimal values for populations of the O(H) and O(H)′ atoms were estimated by comparing R_w values obtained for several sets of populations. Since the z parameters of O(HA)′ and O(HC)′ drifted, they were fixed at the maximum points in the difference Fourier maps calculated by excluding these atoms.

The site of Mn could not be found also in the course of refinement of superstructure. Several cycles of least-squares calculation converged the R value to

0.034 and R_w to 0.034 with anisotropic thermal factors for Cd atoms and isotropic ones for P and O atoms. The weighting scheme employed was the same as that in the refinements of the average structures. The final positional and thermal parameters are given in Table 3*. The R and R_w factors calculated with 746 superlattice reflection data were 0.068 and 0.071, respectively. The $|F_c|^2$ synthesis based on the superlattice reflections gave a map approximately equal to the partial Patterson map. Selected interatomic distances and bond angles are given in Table 4. The superstructure projected on (001) is shown in Fig. 6.

The atomic scattering factors for Cd, P and O, and the correction factors for anomalous scattering were taken from International Tables for X-ray Crystallography (1974).

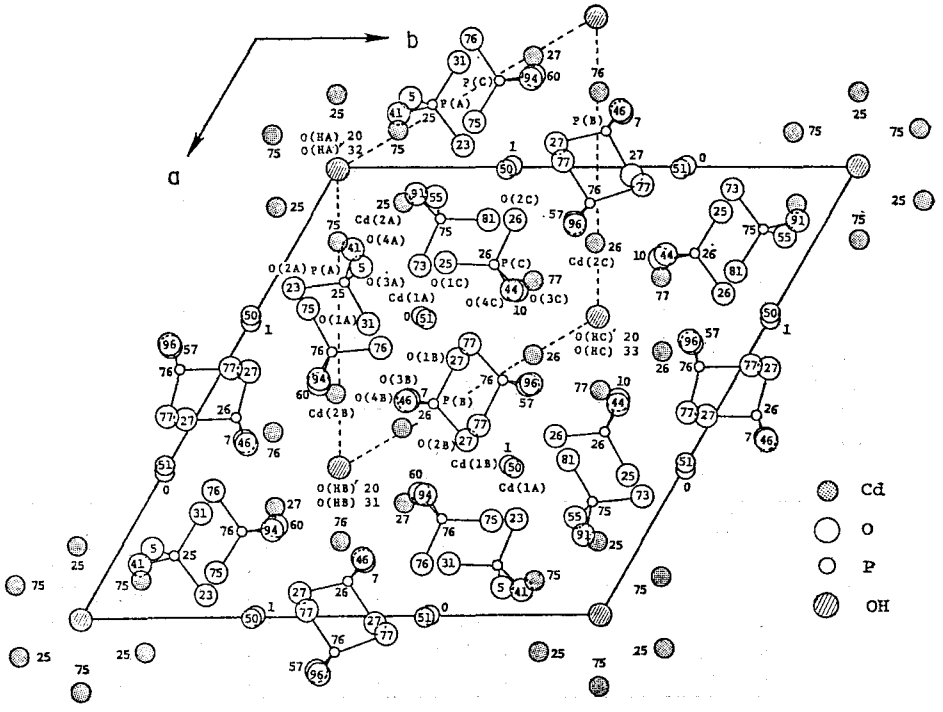

FIG. 6. The superstructure projected on (001). Numbers are $z \times 10^2$. The broken lines represent the unit cell for the average structure.

* Lists of positional and thermal parameters of the average structures for the crystals A, B, C and D, and the observed and calculated structure factors are available on request.

TABLE 3. Positional and thermal parameters for the superstructure.

Positional parameter

	g†	x	y	z	B_{iso}(Å^2)
Cd(1A)	1.0	0.3310(1)	0.3285(1)	0.0020(1)	0.84*
Cd(1B)	1.0	0.6632(1)	0.6609(1)	0.0085(1)	0.92*
Cd(2A)	1.0	0.0791(1)	0.1645(1)	0.2483(1)	0.52*
Cd(2B)	1.0	0.5018(1)	0.2477(1)	0.2655(1)	0.93*
Cd(2C)	1.0	0.1680(1)	0.5806(1)	0.2634(1)	0.99*
P(A)	1.0	0.2554(2)	0.1398(2)	0.2503(5)	0.41(3)
P(B)	1.0	0.5272(2)	0.4471(2)	0.2635(4)	0.33(3)
P(C)	1.0	0.2180(2)	0.4107(2)	0.2603(5)	0.66(4)
O(1A)	1.0	0.3489(5)	0.2330(5)	0.3107(12)	0.14(8)
O(1B)	1.0	0.4287(8)	0.4444(9)	0.2770(16)	1.38(16)
O(1C)	1.0	0.2135(8)	0.3148(8)	0.2560(18)	1.29(14)
O(2A)	1.0	0.2669(6)	0.0504(5)	0.2313(13)	0.49(10)
O(2B)	1.0	0.6091(7)	0.5527(7)	0.2640(15)	1.02(13)
O(2C)	1.0	0.1187(6)	0.4008(6)	0 2593(14)	0.68(11)
O(3A)	1.0	0.2214(6)	0.1574(6)	0.0466(13)	0.40(9)
O(3B)	1.0	0.5156(9)	0.3929(9)	0.0672(20)	1.64(17)
O(3C)	1.0	0.2789(7)	0.4835(7)	0.0982(16)	0.96(12)
O(4A)	1.0	0.1792(6)	0.1212(6)	0.4151(12)	0.30(9)
O(4B)	1.0	0.5196(7)	0.3917(7)	0.4582(14)	0.71(11)
O(4C)	1.0	0.2753(9)	0.4736(9)	0.4397(19)	1.63(16)
O(HA)	0.75	0.0	0.0	0.1953(33)	0.62(26)
O(HA)′	0.25	0.0	0.0	0.315	3.63(225)
O(HB)	0.75	0.6667	0.3333	0.3145(34)	0.78(24)
O(HB)′	0.25	0.6667	0.3333	0.1956(181)	0.78(24)
O(HC)	0.75	0.3333	0.6667	0.3300(28)	0.39(20)
O(HC)′	0.25	0.3333	0.6667	0.195	2.29(123)

Anisotropic temperature factors in the form:

$\exp[-2\pi\{U_{11}h^2a^{*2}+U_{22}k^2b^{*2}+U_{33}l^2c^{*2}+2(U_{12}hka^*b^*+U_{13}hla^*c^*+U_{23}klb^*c^*)\}]$

	U_{11}	U_{22}	U_{33}	U_{12}	U_{13}	U_{23}
Cd(1A)	0.0145(3)	0.0079(3)	0.0062(2)	0.0031(3)	0.0006(4)	−.0020(3)
Cd(1B)	0.0155(3)	0.0095(3)	0.0082(3)	0.0050(3)	−.0029(4)	−.0031(3)
Cd(2A)	0.0100(3)	0.0071(3)	0.0047(2)	0.0060(3)	−.0001(3)	−.0010(3)
Cd(2B)	0.0102(3)	0.0106(3)	0.0125(4)	0.0037(3)	−.0013(3)	−.0001(3)
Cd(2C)	0.0145(4)	0.0116(3)	0.0148(4)	0.0091(3)	0.0015(3)	0.0007(3)

† Population

* Calculated from the anisotropic temperature factors according to the expression; $B_{iso}=4(a^2B_{11}+b^2B_{22}+c^2B_{33}+abB_{12}\cos\gamma)/3$

TABLE 4. Selected interatomic distances (Å) and bond angles (°) for superstructure.

Cd(1A)-O(1A)	2.671(9)	Cd(1B)-O(1A)^{iii}	2.250(9)	Cd(2A)-O(1B)	2.318(9)
-O(1B)	2.530(10)	-O(1B)^{iii}	2.226(10)	-O(2A)^{v}	2.625(11)
-O(1C)	2.471(13)	-O(1C)^{iii}	2.487(12)	-O(3A)	2.720(10)
-O(2A)^{i}	2.413(9)	-O(2A)	2.254(8)	-O(3A)^{vi}	2.251(9)
-O(2B)^{ii}	2.300(13)	-O(2C)	2.381(13)	-O(4A)	2.344(10)
-O(2C)^{i}	2.301(13)	-O(2B)^{iv}	2.277(12)	-O(4A)^{vii}	2.272(8)
-O(3A)	2.450(7)	-O(4A)^{iii}	3.217(7)	-O(HA)	2.335(3)
-O(3B)	2.663(14)	-O(4B)^{iii}	2.661(10)	-O(HA)′	2.351
-O(3C)	3.092(14)	-O(4C)^{iii}	2.840(17)		
Cd(2B)-O(1A)	2.386(9)	Cd(2C)-O(1B)^{xi}	2.397(20)		
-O(2B)^{viii}	2.766(12)	-O(2C)	2.608(10)		
-O(3B)	2.608(15)	-O(3B)^{vi}	2.226(13)		
-O(4B)	2.548(11)	-O(4B)^{vii}	2.208(9)		
-O(3C)^{ix}	2.293(11)	-O(3C)^{xi}	2.321(12)		
-O(4C)^{x}	2.212(13)	-O(4C)^{xi}	2.465(15)		
-O(HB)	2.338(3)	-O(HC)	2.345(3)		
-O(HB)′	2.360(24)	-O(HC)′	2.365		
P(A)-O(1A)	1.564(6)	P(B)-O(1B)	1.576(15)	P(C)-O(1C)	1.517(14)
-O(2A)	1.555(13)	-O(2B)	1.555(12)	-O(2C)	1.533(12)
-O(3A)	1.541(10)	-O(2B)	1.531(14)	-O(3C)	1.537(10)
-O(4A)	1.563(9)	-O(4B)	1.545(10)	-O(4C)	1.594(12)
O(1A)-O(2A)	2.619(11)	O(1B)-O(2B)	2.549(14)	O(1C)-O(2C)	2.535(20)
-O(3A)	2.513(11)	-O(3B)	2.406(22)	-O(3C)	2.607(16)
-O(4A)	2.517(10)	-O(4B)	2.368(19)	-O(4C)	2.589(18)
O(2A)-O(3A)	2.517(12)	O(2B)-O(3B)	2.605(23)	O(2C)-O(3C)	2.489(13)
-O(4A)	2.541(14)	-O(4B)	2.607(20)	-O(4C)	2.536(16)
O(3A)-O(4A)	2.532(11)	O(3B)-O(4B)	2.601(16)	O(3C)-O(4C)	2.341(16)
O(1A)-P(A)-O(2A)	114.2(6)	O(1B)-P(B)-O(2A)	109.0(8)		
O(1A)-P(A)-O(3A)	108.0(4)	O(1B)-P(B)-O(3B)	101.5(7)		
O(1A)-P(A)-O(4A)	107.2(4)	O(1B)-P(B)-O(4B)	98.7(6)		
O(2A)-P(A)-O(3A)	108.7(5)	O(2B)-P(B)-O(3B)	115.2(6)		
O(2A)-P(A)-O(4A)	109.2(5)	O(2B)-P(B)-O(4B)	114.5(5)		
O(3A)-P(A)-O(4A)	109.3(5)	O(3B)-P(B)-O(4B)	115.5(7)		
O(1C)-P(C)-O(2C)	112.4(6)				
O(1C)-P(C)-O(3C)	117.1(7)				
O(1C)-P(C)-O(4C)	112.6(8)				
O(2C)-P(C)-O(3C)	108.3(6)				
O(2C)-P(C)-O(4C)	108.4(7)				
O(3C)-P(C)-O(4C)	96.7(6)				

symmetry code

none	x, y, z	vi	$x-y, x, z+1/2$
i	$1-x, 1-y, z-1/2$	vii	$x-y, x, z-1/2$
ii	$y, y-x, z-1/2$	viii	$1-y, x-y, z$
iii	$1-x, 1-y, z-1/2$	ix	$y, y-x, z+1/2$
iv	$1-y, x-y+1, z$	x	$y, y-x, z-1/2$
v	$-y, x-y, z$	xi	$y-x, 1-x, z$

Discussion

The impurity ions such as Mn^{2+}, Fe^{2+}, Co^{2+}, Ni^{2+}, Cu^{2+} and Hg^{2+} were found to influence the crystal growth and the structure of $Cd_5(PO_4)_3OH$. These elements did not substitute for Cd completely, and the end members for the respective elements could not be obtained under the condition employed in this study. Impurity effects of Fe^{2+}, Co^{2+} and Ni^{2+} on the crystal growth of $Cd_5(PO_4)_3OH$ are similar: they inhibit the growth along [001] direction. Mn^{2+}, Cu^{2+} and Hg^{2+} accelerate the growth of pinacoidal or prismatic faces.

As Klee and Engel (1969) reported, the band corresponding to ν_2 mode of the PO_4 group was not observed on $Cd_5(PO_4)_3OH$ (Fig. 1). The structure analysis revealed that the PO_4 tetrahedron is more distorted in the superstructure than in the structure of $Cd_5(PO_4)_3OH$. A small change of dipole moment due to the slight distortion of the PO_4 groups might give weak bands at 460 and 480 cm^{-1}. Infrared studies on $Ca_5(PO_4)_3OH$ and $Cd_5(PO_4)_3Cl$ crystals containing a small amount of Mn^{2+} or Cu^{2+} revealed that the former crystal gave an additional band at 780 cm^{-1} and the latter at 760 cm^{-1} on introduction of these cations. $Cd_5(PO_4)_3OD$ containing a small amount of Mn^{2+} also showed an additional band at 760 cm^{-1}. Therefore, the band at 760 cm^{-1} is supposed to be due to the metallic ions introduced. Since the internal vibrations of PO_4 groups in various orthophosphates do not appear in the region higher than 1200 cm^{-1}, the band at 1220 cm^{-1} is thought to be a combination of several modes. The relation between formation of the superstructure and appearance of the additional bands is not clear yet.

As shown in Table 2, introduction of Mn^{2+}, Ni^{2+} or Hg^{2+} ions changes the unit cell dimensions of the $Cd_5(PO_4)_3OH$ crystal in the same direction, though Hg^{2+} is larger than Cd^{2+}, and Ni^{2+} and Mn^{2+} are smaller than Cd^{2+}; all of these cations lengthen the *a*-axis and do not cange the *c*-axis significantly. This expansion along the (001) plane is supposed to be caused by the formation of the superstructure.

There are five crystallographically independent Cd atoms in a unit cell of the superstructure. As shown in Fig. 6, the Cd(1A) and Cd(1B) are in six- or nine-coordination, and Cd(2A), Cd(2B) and Cd(2C) are in seven-coordination. The positions of these atoms deviate slightly from those in the average structure. Among the three crystallographically independent PO_4 tetrahedra [$P(A)O_4$, $P(B)O_4$, $P(C)O_4$] the deviations of atomic positions in the $P(A)O_4$ are remarkable. As a consequence, the interatomic distance between O(3A) and Cd(1A) is shorter than those between Cd(1A) and O(1A), O(1B) and O(1C) atoms. Although the $P(A)O_4$ tetrahedron is almost regular, the $P(B)O_4$ and $P(C)O_4$ tetrahedra are much

distorted. The distortion of the $P(A)O_4$ tetrahedron estimated in terms of Baur's *DI*(PO), *DI*(OO) and *DI*(OPO) (Baur, 1974) is a little smaller than that of the PO_4 tetrahedron in the average structure, whereas those of $P(B)O_4$ and $P(C)O_4$ are 2-5 times larger than that in the average structure.

Cadmium hydroxyapatite is tinged with pink on containing a small amount of Mn^{2+}, and becomes purple on containing a larger amount of Mn^{2+}. The intensities of superlattice reflections were found not to be proportional to the amount of Mn^{2+} in the crystal from Weissenberg photographs of several crystals which have different depths of color due to Mn^{2+}. Although little amount of Fe^{2+} or Cu^{2+} substituted for Cd^{2+}, the intensities of superlattice reflections are strong in the crystals grown under existence of such an ion. Further, Weissenberg patterns of these crystals do not depend on the quantity and kind of impurity ions significantly. Single crystals of $Cd_5(PO_4)_3OH$ with the sizes of about 0.5 mm in diameters and 2-3 mm in lengths synthesized in this study showed diffuse streaks at the positions corresponding to those of the superlattice reflections after 48 h (30 kV, 15 mA) exposures. This observation suggests that $Cd_5(PO_4)_3OH$ itself forms a superstructure which has not a three dimensional periodicity. The large anisotropic thermal parameters of O atoms in $Cd_5(PO_4)_3OH$ (Hata *et al.*, 1978) reflect this fact, and the impurity ions might act as a trigger to yield a three dimensional periodicity.

The characteristic thermal vibrations of O atoms in the apatite structures were also observed in $Ca_5(PO_4)_3OH$ (Sudarsanan and Young, 1969) and $Sr_5(PO_4)_3OH$ (Sudarsanan and Young, 1972). Namely, the thermal ellipsoids of the atoms of PO_4 tetrahedra in these crystals drown from the parameters reported by Sudarsanan and Young are quite similar to those of the average structures obtained in the present study. The magnitude of anisotropy is in the order $Cd_5(PO_4)_3OH > Ca_5(PO_4)_3OH > Sr_5(PO_4)_3OH$. The $Ca_5(PO_4)_3OH$ crystals used for structure analysis were natural apatite from Holly Spring, and the $Sr_5(PO_4)_3OH$ crystals were synthesized ones. A little quantity of impurity ions are expected to be contained in the former crystals. Further, since ionic radius of Ca^{2+} is only a little larger than that of Cd^{2+}, an analogous effect of impurity is expected. From these considerations and the results of the infrared studies, it is suggested that $Ca_5(PO_4)_3OH$ also has a possibility to form a superstructure, and that the crystal structure of the biological apatite is expected to be influenced by impurity ions in human body. It can be, therefore, presumed that such a non-centrosymmetric structure takes a part of piezo-electricity of bone.

Acknowledgements—We are very grateful to Professor M. Kato of Tokyo Institute of Technology and to Associate Professor T. Ito of Institute for Molecular

Science, who allowed us to use automated four-circle diffractometers. Thanks are also due to Associate Professor H. Imai of Tokyo Institute of Technology who allowed us to use an infrared spectrometer, to Dr. K. Tanaka for advice in data collection, and to Mr. H. Sakamoto of Kagoshima University for chemical analysis of Hg and Cd. Computations were carried out on the M-180 and M-200 computers (Hitachi) at the Computer Center of Tokyo Institute of Technology and Institute for Molecular Science.

References

BAUR, W.H. (1974) *Acta Cryst.*, **B30**, 1195-1215.
COPPENCE, P & HAMILTON, W.C. (1970) *Acta Cryst.*, **A26**, 71-83.
HATA, M., OKADA, K., AKAO, M., AOKI, H. & IWAI, S. (1978) *Acta Cryst.*, **B34**, 3062-3064.
HUGHES, E.W. (1974) *Journ. Amer. Chem. Soc.*, **63**, 1737-1752.
International Tables for X-ray Crystallography (1974) Vol. 4., Kynoch Press, Birmingham.
ITO, T. (1973) *Zeits. Krist.*, **137**, 399-411.
KLEE, W.E. & ENGEL, G. (1969) *Journ. inorg. nucl. Chem.*, **32**, 1837-1843.
KREIDER, E.R. & HUMMEL, F.A. (1970) *Amer. Miner.*, **55**, 170-184.
MEHMEL, M., (1930) *Zeits. Krist.*, **75**, 323-331.
NÁRAY-SZABÓ, S. (1930) *Zeits. Krist.*, **75**, 387-398.
PRENER, J.S. (1967) *Journ. Electrochem. Soc.*, **114**, No. 1, 77-83.
SAKURAI, T. (1967) *Universal Program System for Crystallographic Computation*. Cryst. Soc. Japan.
SHANNON, R.D. (1976) *Acta Cryst.*, **A32**, 751-767.
SUDARSANAN, K. & YOUNG, R.A. (1969) *Acta Cryst.*, **B25**, 1534-1543.
SUDARSANAN, K. & YOUNG, R.A. (1972) *Acta Cryst.*, **B28**, 3668-3670.
TAKENAKA, A. (1972) *Schematic Drawing of Crystal and Molecular Structures Containing Atomic Thermal Motions*. APPLY270/23-503-001, Tokyo Fujitsu Ltd.

Received January 4, 1983.